# Analytical ultracentrifugation and preliminary X-ray studies of the chloroplast envelope quinone oxidoreductase homologue from Arabidopsis thaliana.

Sarah Mas y Mas, Cécile Giustini, Jean-Luc Ferrer, Norbert Rolland, Gilles Curien, David Cobessi

▶ **To cite this version:**

HAL is a multi-disciplinary open access archive for the deposit and dissemination of scientific research documents, whether they are published or not. The documents may come from teaching and research institutions in France or abroad, or from public or private research centers.

L'archive ouverte pluridisciplinaire **HAL**, est destinée au dépôt et à la diffusion de documents scientifiques de niveau recherche, publiés ou non, émanant des établissements d'enseignement et de recherche français ou étrangers, des laboratoires publics ou privés.

# Analytical ultracentrifugation and preliminary X-ray studies of the chloroplast envelope quinone oxidoreductase homologue from *Arabidopsis thaliana*

**Sarah Mas y mas,[a] Cécile Giustini,[b] Jean-Luc Ferrer,[c] Norbert Rolland,[b] Gilles Curien[b] and David Cobessi[d]***
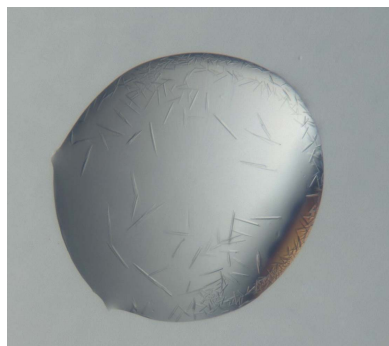
[a]Institut de Biologie Structurale, Université Grenoble Alpes, CNRS, CEA, 71 Avenue des Martyrs, 38044 Grenoble, France, [b]Laboratoire de Physiologie Cellulaire et Végétale, CNRS, Université Grenoble Alpes, CEA, INRA, 17 Rue des Martyrs, 38054 Grenoble, France, [c]Institut de Biologie Structurale, CEA, Université Grenoble Alpes, CNRS, 71 Avenue des Martyrs, 38044 Grenoble, France, and [d]Institut de Biologie Structurale, CNRS, Université Grenoble Alpes, CEA, 71 Avenue des Martyrs, 38044 Grenoble, France. *Correspondence e-mail: david.cobessi@ibs.fr

Quinone oxidoreductases reduce a broad range of quinones and are widely distributed among living organisms. The chloroplast envelope quinone oxidoreductase homologue (ceQORH) from *Arabidopsis thaliana* binds NADPH, lacks a classical N-terminal and cleavable chloroplast transit peptide, and is transported through the chloroplast envelope membrane by an unknown alternative pathway without cleavage of its internal chloroplast targeting sequence. To unravel the fold of this targeting sequence and its substrate specificity, ceQORH from *A. thaliana* was overexpressed in *Escherichia coli*, purified and crystallized. Crystals of apo ceQORH were obtained and a complete data set was collected at 2.34 Å resolution. The crystals belonged to space group $C222_1$, with two molecules in the asymmetric unit.

## 1. Introduction

The chloroplast plays central roles in plant growth and development by catalyzing a remarkable range of metabolic and physiological functions (Armbruster *et al.*, 2009; Rolland *et al.*, 2012). Most of the chloroplast proteins are encoded by the nuclear genome, synthesized in the cytosol and then imported into the chloroplast through the TOC/TIC (translocons at the outer and inner envelope of the chloroplast) machineries (Strittmatter *et al.*, 2010). If most of the outer envelope proteins are excluded, these chloroplast proteins possess a predictable and cleavable transit peptide at their N-terminus (Jarvis & López-Juez, 2013; Richardson *et al.*, 2014). Recently, some chloroplast proteins, such as the inner envelope protein IEP32, also called Tic32 (Nada & Soll, 2004), and the chloroplast envelope quinone oxidoreductase homologue (ceQORH; Miras *et al.*, 2002, 2007), have been shown to be targeted to the chloroplast inner envelope membrane while lacking this predictable and cleavable transit peptide. Moreover, the two abovementioned chloroplast proteins were also shown to be targeted to the chloroplast by an as yet unknown alternative targeting pathway (Miras *et al.*, 2007).

While information for the targeting of canonical chloroplast proteins is located at their N-terminus (*i.e.* within the transit peptide sequence), ceQORH displays a nonterminal hydrophilic domain (residues 59–100) that is essential for its targeting to the chloroplast (Miras *et al.*, 2007). Based on sequence alignment, the 329-residue ceQORH protein was proposed to belong to the quinone oxidoreductase (QOR)

**Table 1**
Macromolecule-production information.

| | |
|---|---|
| Source organism | *A. thaliana* |
| DNA source | AT4G13010 cDNA |
| Cloning vector | pET-30a+ |
| Expression vector | pET-30a+ |
| Expression host | *E. coli* Rosetta2 (DE3) |
| Complete amino-acid sequence of the construct produced | AGKLMHALQYNSYGGGAAGLEHVQVPVPTPKSNE-VCLKLEATSLNPVDWKIQKGMIRPFLPRKFPC-IPATDVAGEVVEVGSGVKNFKAGDKVVAVLSH-LGGGGLAEFAVATEKLTVKRPQEVGAAEAAAL-PVAGLTALQALTNPAGLKLDGTGKKANILVTA-ASGGVGHYAVQLAKLANAHVTATCGARNIEFV-KSLGADEVLDYKTPEGAALKSPSGKKYDAVVH-CANGIPFSVFEPNLSENGKVIDITPGPNAMWT-YAVKKITMSKKQLVPLLLIPKAENLEFMVNLV-KEGKVKTVIDSKHPLSKAEDAWAKSIDGHATG-KIIVEP |

**Table 2**
Crystallization.

| | |
|---|---|
| Method | Hanging drop |
| Plate type | Linbro plate |
| Temperature (K) | 293 |
| Protein concentration (mg ml$^{-1}$) | 5 |
| Buffer composition of protein solution | 50 m$M$ Tris–HCl pH 7.5, 200 m$M$ KCl, 2 m$M$ DTT, 1 m$M$ EDTA, 10% glycerol |
| Composition of reservoir solution | 0.2 $M$ sodium acetate, 0.1 $M$ Tris–HCl pH 8.5, 32%($v/v$) PEG 4000 |
| Volume and ratio of drop | 2 µl + 2 µl |
| Volume of reservoir (µl) | 500 |

family (Miras *et al.*, 2002). This enzyme family shares common structural motifs and oxidizes NADPH to reduce a broad range of quinones, and is widely distributed among living organisms (Pan *et al.*, 2009). Enzymes belonging to the quinone oxidoreductase (QOR) family are often dimeric, such as those from *Escherichia coli* (Thorn *et al.*, 1995) and *Saccharomyces cerevisiae* (Guo *et al.*, 2011), but can also be monomeric, such as that from *Coxiella burnetii*, which is the only known structure of a monomeric QOR (PDB entry 3tqh; M. C. Franklin, J. Cheung, M. Rudolph, M. Cassidy, E. Gary, F. Burshteyn & J. Love, unpublished work). No significant sequence identity is observed between the region corresponding to the transit peptide of ceQORH and the QOR sequences of known structures. Recently, ceQORH has also been reported to bind calmodulin (CaM; Dell'Aglio *et al.*, 2013), as does IEP32 (Chigri *et al.*, 2006), a property that has never been reported for other QORs.

In order to unravel the structural characteristics of the uncleaved transit peptide and to obtain insights into the substrate specificity and binding of CaM to ceQORH, we undertook structural studies of this protein. Here, we report the cloning, purification and crystallization of ceQORH from *Arabidopsis thaliana* and data collection from crystals of the apo form. Analytical ultracentrifugation studies are also discussed.

## 2. Materials and methods

### 2.1. Macromolecule production

**2.1.1. Protein expression and purification.** The AT4G13010 cDNA coding for a 329-amino-acid protein was inserted into a pET-30a+ vector to transform *E. coli* Rosetta2 (DE3) cells. The cells were grown overnight in 20 ml LB with 30 µg ml$^{-1}$ kanamycin and 34 µg ml$^{-1}$ chloramphenicol at 37°C. This first culture was used to inoculate 2 l LB (with antibiotics). Growth was continued at 37°C. When the OD$_{600}$ reached 0.6, the temperature was decreased to 20°C and 0.4 m$M$ isopropyl $\beta$-D-1-thiogalactopyranoside (IPTG) was added. After overnight induction, the bacteria were harvested by centrifugation at 5500$g$ for 30 min at 4°C. The cell pellet was suspended in 50 ml lysis buffer [50 m$M$ Tris–HCl pH 7.5, 1 m$M$ EDTA, 1 m$M$

DTT, 10%($v/v$) glycerol]. A cOmplete protease-inhibitor cocktail tablet (Roche) and, after lysis, 0.2%($w/v$) streptomycin sulfate were added. The lysate was centrifuged at 14 000$g$ for 30 min at 4°C. The purification was performed at 4°C. The supernatant was applied onto a DEAE Sepharose column in 50 m$M$ Tris–HCl pH 7.5, 5 m$M$ DTT, 1 m$M$ EDTA, 10%($v/v$) glycerol. ceQORH displays a high theoretical isoelectric point (pI = 9.05) and thus eluted in the flow through. It was collected, concentrated and applied onto an SP Sepharose column. ceQORH was eluted with a linear gradient to 50 m$M$ Tris–HCl pH 7.5, 1 $M$ KCl, 5 m$M$ DTT, 1 m$M$ EDTA, 10%($v/v$) glycerol. The fractions containing ceQORH eluted between 150 and 180 m$M$ KCl. They were pooled and concentrated with an Amicon Ultra 4 ml centrifugal filter with a 10 kDa membrane cutoff; they were then loaded onto a HiLoad 16/60 Superdex 200 column and eluted with 50 m$M$ Tris–HCl pH 7.5, 200 m$M$ KCl, 2 m$M$ DTT, 1 m$M$ EDTA, 10%($v/v$) glycerol. The pool containing pure ceQORH was concentrated and frozen in liquid nitrogen before use. Macromolecule-production information is summarized in Table 1.

**2.1.2. Analytical ultracentrifugation.** The analytical ultracentrifugation experiment was performed with an Proteome-Lab XL-I analytical ultracentrifuge from Beckman Coulter (Palo Alto, USA) and an An-60 Ti rotor (Beckman Coulter). The cells had a double sector (Nanolytics) with optical routes of either 12, 3 or 1.5 mm and were equipped with Sapphire windows. Absorbance and interference measurements were performed with the *ProteomeLab XL-I* v.6.0 software. The samples were prepared at 0.6 and 6.0 mg ml$^{-1}$ in 10 m$M$ Tris–HCl pH 7.5, 150 m$M$ NaCl (AUC buffer) supplemented with NADPH (1.45 m$M$) as indicated in Supplementary Table S1. The interference and absorbance were recorded for 12 h at 50 000 rev min$^{-1}$ at 20°C. ceQORH was considered to be a compact spherical protein (molecular weight 34 304 Da) with $\overline{v} = 0.745$ ml g$^{-1}$, $f/f_{min} = 1.25$, $\rho = 1.005$ g ml$^{-1}$ and $\eta = 1.02$ cP at a temperature of 20°C. Using these parameters, the sedimentation coefficient was estimated by *SEDNTERP* assuming several oligomerization states (Supplementary Table S2). Data analysis was performed with *SEDFIT* v.14.c.

### 2.2. Crystallization

ceQORH at 5 mg ml$^{-1}$ in 50 m$M$ Tris–HCl pH 7.5, 200 m$M$ KCl, 2 m$M$ DTT, 1 m$M$ EDTA, 10%($v/v$) glycerol was subjected to crystallization in its apo form using the sitting-

drop vapour-diffusion technique and the high-throughput crystallization facility at EMBL, Grenoble at 4°C. Crystallization hits were optimized using Linbro plates at 20°C. Crystallization information is summarized in Table 2.
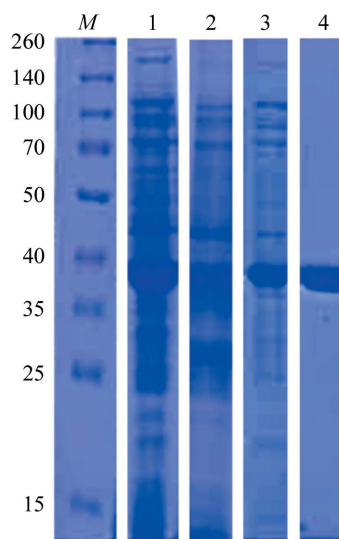
### 2.3. Data collection and processing

Diffraction data were collected on beamline FIP-BM30A (Roth *et al.*, 2002) at the European Synchrotron Radiation Facility (ESRF), Grenoble, France at a wavelength of 0.9800 Å at 100 K using an ADSC 315r detector. The crystal-to-detector distance was 412.20 mm. The data were processed and scaled using *XDS* (Kabsch, 2010).

### 3. Results and discussion

#### 3.1. Purification and analytical ultracentrifugation

After overnight expression, ceQORH was found mainly in the soluble fraction. Most of the contaminants were eliminated using a DEAE Sepharose column (Fig. 1). Two peaks of ceQORH with different $OD_{260}/OD_{280}$ ratios were obtained from the SP Sepharose column, suggesting that ceQORH in one of these peaks is bound to nucleic acids or other absorbing molecules. The peak with the lower $OD_{260}/OD_{280}$ ratio was selected and subjected to gel filtration. Pure protein was obtained with a yield of 14 mg per litre of culture. Analysis of the AUC sedimentation results for apo ceQORH showed numerous peaks between 2 and 10 S (Fig. 2a) corresponding to monomer, dimer and tetramer and possible aggregation at the two protein concentrations. When NADPH was added, only one peak at $2.7 \pm 0.1$ S ($s_{20,w} = 2.8$ S) was observed and the fri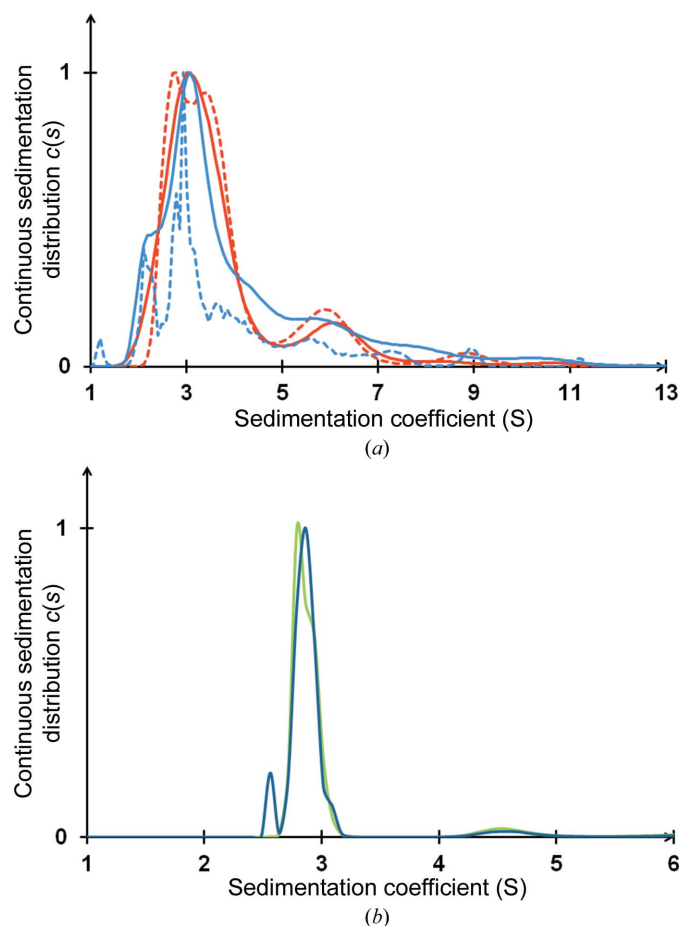ctional ratio was 1.27. The theoretical frictional ratio for a globular monomeric protein is 1.25 (Fig. 2b). Therefore, ceQORH–NADPH is monomeric (Supplementary Table S3). The results suggest that ceQORH undergoes a conformational change upon NADPH binding, leading to a transition from a dimer or a tetramer to a monomer.

#### 3.2. Crystallization and data collection

Crystallization trials with ceQORH–NADPH failed even though this enzyme form was monodisperse in solution. These results suggest that ceQORH bound to NADPH is probably flexible and prevents crystal nucleation and growth. This is a difference from other QORs, since crystals of QOR from *E. coli* or *S. cerevisiae* bound to NADP⁺ or of QOR from *C. burnetii* bound to NADPH were obtained. Surprisingly, apo ceQORH crystallized in the presence of 0.2 *M* sodium acetate, 0.1 *M* Tris–HCl pH 8.5, 32%(*v/v*) PEG 4000, as according to the AUC result apo ceQORH has different oligomeric states in solution. A complete X-ray diffraction data set was collected to 2.34 Å resolution from a crystal of apo ceQORH (Fig. 3). The crystals belonged to the orthorhombic system, with unit-cell parameters $a = 44.72$, $b = 142.65$, $c = 209.89$ Å.



**Figure 1**
Purification of recombinant *A. thaliana* ceQORH. Proteins were separated on a 12% SDS–PAGE stained with Coomassie Brilliant Blue R-250. Lane *M*, molecular-weight markers (labelled in kDa); lane 1, crude soluble extract; lane 2, flow through from the DEAE Sepharose column containing ceQORH; lane 3, pool of the fractions containing ceQORH eluted from the SP Sepharose column; lane 4, fraction containing ceQORH eluted from the gel-filtration column.
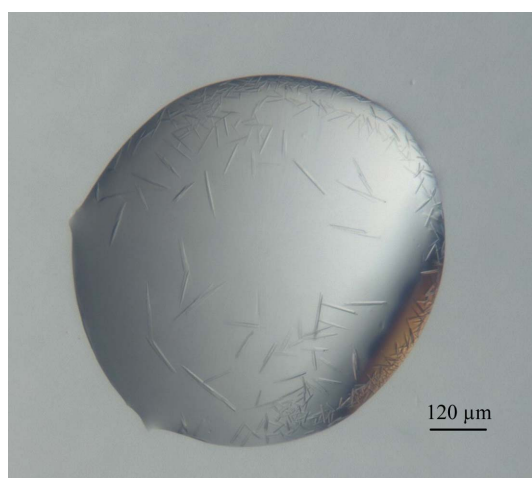


**Figure 2**
(*a*) Sedimentation curves of ceQORH calculated from absorbance (solid line) and interference (dashed lines) measurements for two ceQORH concentrations: 6 mg ml⁻¹ (red) and 0.6 mg ml⁻¹ (blue). (*b*) Sedimentation curves of ceQORH–NADPH calculated from absorbance (green) and interference (blue) experiments (ceQORH concentration 6 mg ml⁻¹; NADPH concentration 1.45 m*M*).

**Table 3**
Data collection and processing.

Values in parentheses are for the outer shell.

| | |
|---|---|
| Diffraction source | FIP-BM30A, ESRF |
| Wavelength (Å) | 0.9800 |
| Temperature (K) | 100 |
| Detector | ADSC 315r |
| Crystal-to-detector distance (mm) | 412.20 |
| Rotation range per image (°) | 0.75 |
| Rotation range (°) | 180 |
| Mosaicity (°) | 0.13 |
| Space group | $C222_1$ |
| $a, b, c$ (Å) | 44.72, 142.65, 209.89 |
| $\alpha, \beta, \gamma$ (°) | 90, 90, 90 |
| Resolution range (Å) | 41.82–2.34 (2.49–2.34) |
| Total No. of reflections | 172766 (13536) |
| No. of unique reflections | 28220 (4078) |
| Completeness (%) | 97.9 (88.9) |
| Multiplicity | 6.12 (3.31) |
| $\langle I/\sigma(I)\rangle$ | 13.03 (2.62) |
| $R_{meas}$ (%) | 13.20 (45.30) |



**Figure 3**
ceQORH crystals obtained at 4°C using 0.2 $M$ sodium acetate, 0.1 $M$ Tris–HCl pH 8.5, 32% PEG 4000 with the protein at 5 mg ml$^{-1}$.

Data statistics are summarized in Table 3. Systematic extinctions along the 00*l* axis showed that the crystals belonged to space group $C222_1$. Solvent-content analysis suggests that two molecules are present in the asymmetric unit, with a solvent content of 45.8%. Analysis of the self-rotation function reveals the presence of a peak corresponding to a noncrystallographic twofold axis ($\kappa = 180$, $\omega = 55$, $\varphi = 155°$). Therefore, a dimer of apo ceQORH is present in the asymmetric unit.

Ligand screening to study the activity of the protein has been undertaken. Combined with X-ray crystallography, these studies should provide new insights into the ligand-binding specificity, protein–protein interaction (CaM binding) and the structure of the internal transit peptide sequence.

## References

Armbruster, U., Hertle, A., Makarenko, E., Zühlke, J., Pribil, M., Dietzmann, A., Schliebner, I., Aseeva, E., Fenino, E., Scharfenberg, M., Voigt, C. & Leister, D. (2009). *Mol. Plant*, **2**, 1325–1335.

Chigri, F., Hörmann, F., Stamp, A., Stammers, D. K., Bölter, B., Soll, J. & Vothknecht, U. C. (2006). *Proc. Natl Acad. Sci. USA*, **103**, 16051–16056.

Dell'Aglio, E., Giustini, C., Salvi, D., Brugière, S., Delpierre, F., Moyet, L., Baudet, M., Seigneurin-Berny, D., Matringe, M., Ferro, M., Rolland, N. & Curien, G. (2013). *Mol. Biosyst.* **9**, 1234–1248.

Guo, P.-C., Ma, X.-X., Bao, Z.-Z., Ma, J.-D., Chen, Y. & Zhou, C.-Z. (2011). *J. Struct. Biol.* **176**, 112–118.

Jarvis, P. & López-Juez, E. (2013). *Nature Rev. Mol. Cell Biol.* **14**, 787–802.

Kabsch, W. (2010). *Acta Cryst.* D**66**, 133–144.

Miras, S., Salvi, D., Ferro, M., Grunwald, D., Garin, J., Joyard, J. & Rolland, N. (2002). *J. Biol. Chem.* **277**, 47770–47778.

Miras, S., Salvi, D., Piette, L., Seigneurin-Berny, D., Grunwald, D., Reinbothe, C., Joyard, J., Reinbothe, S. & Rolland, N. (2007). *J. Biol. Chem.* **282**, 29482–29492.

Nada, A. & Soll, J. (2004). *J. Cell Sci.* **117**, 3975–3982.

Pan, X., Zhang, H., Gao, Y., Li, M. & Chang, W. (2009). *Biochem. Biophys. Res. Commun.* **390**, 597–602.

Richardson, L. G. L., Paila, Y. D., Siman, S. R., Chen, Y., Smith, M. D. & Schnell, D. J. (2014). *Front. Plant Sci.* **5**, 269.

Rolland, N., Curien, G., Finazzi, G., Kuntz, M., Maréchal, E., Matringe, M., Ravanel, S. & Seigneurin-Berny, D. (2012). *Annu. Rev. Genet.* **46**, 233–264.

Roth, M., Carpentier, P., Kaïkati, O., Joly, J., Charrault, P., Pirocchi, M., Kahn, R., Fanchon, E., Jacquamet, L., Borel, F., Bertoni, A., Israel-Gouy, P. & Ferrer, J.-L. (2002). *Acta Cryst.* D**58**, 805–814.

Strittmatter, P., Soll, J. & Bölter, B. (2010). *Methods Mol. Biol.* **619**, 307–321.

Thorn, J. M., Barton, J. D., Dixon, N. E., Ollis, D. L. & Edwards, K. J. (1995). *J. Mol. Biol.* **249**, 785–799.